Environmental Science
Water Research & Technology

Optical Properties and Photochemical Production of Hydroxyl Radical and Singlet Oxygen after Ozonation of Dissolved Organic Matter

Journal:	*Environmental Science: Water Research & Technology*
Manuscript ID	EW-ART-09-2020-000878.R1
Article Type:	Paper

Water impact statement

Water treatment tends towards increasingly numerous treatment steps. A better understanding of the effects of ozonation on the optical and photochemical properties of dissolved organic matter is necessary to optimize treatment processes. Ozonation induces a decrease in light absorbance and can help downstream UV-based treatment steps or for wastewater leads to improvements of the aesthetics of the water.

Optical Properties and Photochemical Production of Hydroxyl Radical and Singlet Oxygen after Ozonation of Dissolved Organic Matter

Frank Leresche [¤,⊥], Jeremy A. Torres-Ruiz [†], Tyler Kurtz[⊥], Urs von Gunten[#,‡], and Fernando L. Rosario-Ortiz [¤,⊥,*]

[⊥]Environmental Engineering Program, University of Colorado Boulder, Colorado 80309, United States

[¤] Department of Civil, Environmental and Architectural Engineering, University of Colorado Boulder, Colorado 80309, United States

[†]Department of Chemistry, University of Puerto Rico, Mayagüez, Puerto Rico 00682, United States

[#] Eawag, Swiss Federal Institute of Aquatic Science and Technology, Überlandstrasse 133, CH-8600 Dübendorf, Switzerland

[‡]School of Architecture, Civil and Environmental Engineering (ENAC), Ecole Polytechnique Fédérale de Lausanne (EPFL), CH-1015 Lausanne, Switzerland

[*] Corresponding author: Fernando.rosario@colorado.edu

Abstract

This study focuses on the effects of ozonation on the optical and photochemical properties of dissolved organic matter (DOM). Upon ozonation, a decrease in light absorption properties of DOM was observed concomitantly with a large increase in singlet oxygen ($^1O_2$) and hydroxyl radical ($^{\bullet}OH$) quantum yields (Φ_{1O2} and $\Phi_{^{\bullet}OH}$, respectively). The decrease in absorbance was linked to the reaction of DOM chromophores with ozone and $^{\bullet}OH$, formed as a secondary oxidant, while the increase in Φ_{1O2} and $\Phi_{^{\bullet}OH}$ are linked to the formation of quinone-like moieties from the reaction of ozone with phenolic DOM moieties. Investigations using benzoic acid as a $^{\bullet}OH$ probe and methanol as a $^{\bullet}OH$ scavenger indicated that not only is $^{\bullet}OH$ formed, but that other hydroxylating species ($^{\bullet}OH$-like) are also produced upon DOM photo-irradiation.

Introduction

Ozonation is a process widely applied in drinking water treatment and more recently also as a polishing step in secondary effluents of municipal wastewater treatment plants.(1, 2) In addition to its use as a disinfectant and for the oxidation of micropollutants, ozone reacts with the dissolved organic matter (DOM) present in the water, leading to changes in its physico-chemical properties.(3-5) Because wastewater is usually discharged to a receiving water body (e.g., river, lake, sea) and can represent an important fraction of the receiving water, ozone-induced transformations of DOM are of interest.(6, 7)

DOM plays an important role in the photo-transformation of contaminants in surface waters by absorbing a portion of sunlight, thereby decreasing the direct photo-transformation of contaminants (equation 1), and by producing reactive intermediates (RI). These RI include excited triplet state of the DOM (^{3}DOM*, equation 2), singlet oxygen ($^1O_2$, equation 3) and hydroxyl radical ($^\bullet$OH, equation 4, where DOM' represents a transformed chromophore of DOM). The RI can react with contaminants leading to transformation products (equation 5).(8-12) Ozonation of DOM will affect this photochemistry by changing the light absorption properties of DOM and potentially affecting the yields of the RI.(3)

$$\text{Contaminant} + h\nu \rightarrow \text{Products} \quad (1)$$

$$\text{DOM} + h\nu \rightarrow {}^1\text{DOM}^* \rightarrow {}^3\text{DOM}^* \quad (2)$$

$$ {}^3\text{DOM}^* + O_2 \rightarrow \text{DOM} + {}^1O_2 \quad (3)$$

$$\text{DOM} + h\nu \rightarrow \text{DOM'} + {}^\bullet\text{OH} \quad (4)$$

$$({}^1O_2 \text{ or } {}^3\text{DOM}^* \text{ or } {}^\bullet\text{OH}) + \text{Contaminant} \rightarrow \text{Products} \quad (5)$$

Studies have shown that ozonation of DOM leads to changes in its physicochemical properties, including decreases in light absorption, fluorescence intensity, chemical oxygen demand, and electron donating capacity, as well as the formation of low molecular weight compounds such as carboxylic acids and aldehydes.(1, 3, 4, 13, 14) DOM moieties have a large range of reactivity towards ozone. DOM moieties with high ozone reactivities are believed to be mostly phenolic compounds that react to quinones, ketones, catechol, and ring opening products.(15, 16) Ozone reactions with DOM were covered in recent publications and we refer the reader to those for more information.(3, 4) Reaction of ozone with DOM forms $^{\bullet}OH$ as a side product that can further react with the DOM.(17-19) $^{\bullet}OH$ reacts with aromatic or conjugated DOM moieties by $^{\bullet}OH$ addition or with unsaturated moieties by $H^{\bullet}$ abstraction.(1) Typical second order rate constants for $^{\bullet}OH$ addition reactions are between $1\text{-}10\times10^{9}$ M^{-1} s^{-1} and are relatively faster than $H^{\bullet}$ abstraction reactions, with typical second order rate constants in the range of $0.1\text{-}1\times10^{9}$ M^{-1} s^{-1}.(20)

In a previous publication, we discussed the effects of ozone on the optical properties of DOM and its effect on the photochemical generation of $^1O_2$.(3) Specifically, it was shown that during ozonation in the presence of *t*-butanol to quench $^{\bullet}OH$ (formed via ozone decomposition), both the fluorescence and $^1O_2$ quantum yield (Φ_{1O2}) increased concomitantly. The fluorescence quantum yield increased by 92-111% for increasing specific ozone doses from 0 to 1 $mmol_{O3}$ $mmol_C^{-1}$. Similarly, the Φ_{1O2} increased by 273-844%. In this previous publication it was hypothesized that this was due to the preferential reactions of ozone with phenolic DOM moieties and low fluorescence chromophores. This hypothesis is based on the following observations: (1) Ozone reacts towards DOM faster at high pH than at low pH.(4) This can be explained by the reaction of ozone towards phenolate being several orders of magnitude faster

than towards phenols (e.g. $k_{O3,\ phenolate}$ = 1.4×10^9 M^{-1} s^{-1} vs $k_{O3,\ phenol}$ = 1.3×10^3 M^{-1} s^{-1} (1)). (2) The aforementioned formation of quinones from ozonation of phenols. (3) The fact that phenols have low Φ_{1O2} (1-6%) (21) while quinones have generally higher Φ_{1O2} (20-98%).(22-25) (4) Low ozone doses can induce an increase in $^1O_2$ production rate. (3) It should be noted that ref. (3) attributes the observed increase in fluorescence quantum yield upon DOM ozonation to a preferential ozone reaction towards chromophores absorbing at long wavelengths that have low fluorescence quantum yields. Such preferential reactions of ozone with chromophores absorbing at long wavelengths may also explain part of the observed increase in Φ_{1O2}. However, given the magnitude of the effect, it cannot be the sole explanation for the observed increase in Φ_{1O2}.

The goal of this study is to expand on our earlier work and investigate the impact of ozone on the photochemical formation of •OH from DOM. Specifically, this paper focuses on the effects of ozonation on (1) the optical properties of DOM, such as the absorbance spectra and of parameters that can be derived from the absorbance, and (2) the potential of DOM to generate singlet oxygen ($^1O_2$) and hydroxyl radical (•OH) under simulated sunlight irradiation. In this study, we evaluated the impact of ozone *without* a •OH quencher, therefore, providing a realistic depiction of the expected effects during the application of ozone in engineered systems. In addition to these effects of ozone, this paper also provides new insights on the molecular composition of DOM.

92 # Materials and Methods

93 ## Analytical instrumentation

94 UV-Vis spectra and absorbance were measured on a Cary 100 Bio UV-Visible
95 spectrophotometer using 0.2, 1, or 5 cm pathlength quartz cuvettes. The pH was measured using
96 a calibrated Orion Star A211 pH-meter using a Thermo Scientific Orion pH electrode model
97 8157BNUMD.

98 Following the photo-irradiation experiments, concentrations of the probe compounds and
99 of the actinometer were measured in duplicate using an Agilent 1200 high-performance liquid
100 chromatography (HPLC) system equipped with a UV-Vis detector, a fluorescence detector and
101 an Agilent Eclipse Plus C-18 5μm particle size reverse phase column. Details of the applied
102 isocratic method are provided in Table S1 of the electronic supplementary information (ESI).

103 ## Chemicals and solutions

104 Chemicals were used as received except for *p*-nitroanisole (PNA), which was recrystallized
105 in hexane, and benzoic acid (BA), which was recrystallized in water to remove some salicylic
106 acid (SA) impurities from the commercially available product. For a complete list of chemicals,
107 refer to Text S1 (ESI). All solutions were prepared in ultrapure water (resistivity 18.2 MΩ cm)
108 obtained from a Sartorios Stedim or equivalent dispenser. A 100 mM buffer stock solution was
109 prepared by adding the appropriate amount of sodium phosphate salts. Diluted 1/10 v/v with
110 water, it resulted in a 10 mM pH 7 phosphate buffer used for the experiments.

111 Two DOM isolates were selected from the International Humic Substance Society (IHSS,
112 St-Paul, MN, USA) as representative of autochthonous (Pony Lake fulvic acid (PLFA), 1R109F)
113 and allochthonous (Suwannee River fulvic acid (SRFA), 1S101F) DOM. The carbon content of

the DOM solutions was measured spectrophotometrically using the specific ultraviolet absorbance value at the wavelength λ=254 nm ($SUVA_{254}$) of 4.2 and 2.5 L mg_C^{-1} m^{-1} for SRFA and PLFA, respectively.(5) Stock solutions of the two DOM types were prepared at concentrations of ≈50mg_C L^{-1} in pH 7 buffer. After stirring for 3-4 hours, the stock solutions were filtered by ultrapure water prewashed 0.45μm pore size polyethersulfone filters (Whatman) and the carbon content was then measured spectrophotometrically.

Ozonation experiments

An ozone/oxygen gas mixture was obtained from an Ozone Solutions ozone generator model TG-40 and bubbled in a cooled (2°C) 2 L cylindrical vessel filled with ultrapure water. An aqueous ozone stock solution with an ozone concentration of ≈1 mM was obtained and was measured using a 0.2 cm path length quartz cuvette on the aforementioned spectrophotometer and a molar absorption coefficient value of 3200 M^{-1} cm^{-1} at λ=260nm.(1) The ozone solution was then added to buffered (pH 7, using the aforementioned phosphate buffer) DOM solutions (final concentration 5 mg_C L^{-1}) at various specific ozone doses (≤1 $mmol_{O3}$ $mmol_C^{-1}$) and the solutions were kept for a minimum of 2 days at 4°C to allow ozone to react to completion. The specific ozone doses were chosen to be similar to those used in drinking water or wastewater facilities.(26-29) It should be noted that for the specific ozone doses of 0.75 and 1 $mmol_{O3}$ $mmol_C^{-1}$ only the UV-vis absorbance spectra are presented. These two doses have low absorbance values (< 0.01 at λ=350nm) that could suffer from systematic errors on the absorbance measurements and we decided not to use them for further calculations.

Irradiation experiments

The methods to determine $^1O_2$ steady-state concentration ($[^1O_2]_{ss}$) and quantum yield (Φ_{1O2}) are described elsewhere.(3) Briefly, $[^1O_2]_{ss}$ during photoirradiation of the ozonated DOM

solutions was measured by spiking the solution with 22.5 μM of furfuryl alcohol (FFA) and 0.1 M of methanol (to quench •OH). At this FFA concentration, $^1O_2$ is mostly (≈99%) deactivated by collision with water and the presence of FFA does not affect but allows to determine the $[^1O_2]_{ss}$.(30) The solutions were then irradiated in 5 mL glass vials in a Rayonet photo-reactor model RPR-100 equipped with 16 RPR-3500A lamps that had an emission spectrum centered around 366 nm (see Figure S1 (ESI) for an emission spectrum of the lamps). 100 μL aliquots were taken at regular time intervals (total irradiation time ≈1 hour), diluted 1/1 (v/v) with ultrapure water and subsequently the FFA concentration was analyzed by HPLC. The abatement of FFA was fitted to a first-order kinetic model using the software Origin 2018. The steady-state concentration of $^1O_2$ ($[^1O_2]_{ss}$) during the experiments was determined using the second-order rate constant $k_{FFA,1O2}$ of $(1.00\pm0.04)\times10^8$ M^{-1} s^{-1}.(31) Φ_{1O2} was then determined by dividing $[^1O_2]_{ss}$ by the rate of light absorption.

The experiments to determine the production rate of •OH and the $\Phi_{\bullet OH}$ where conducted similarly as for the determination of $^1O_2$ and are described in Text S2 (ESI). Briefly, we spiked the samples with 1 mM of BA and the •OH production was determined by following the zero-order production of SA from the reaction of BA with •OH using the yield of the reaction of BA + •OH → SA of 15.5%.(32) For the experiments that used both BA and methanol as •OH probes, the experiment's irradiation time was relatively longer due to the overall lower rate of SA production and we observed a small (≈10% in control experiments containing the ozonated DOMs, 100 nM SA and 0.01 M methanol, irradiated for 225 minutes) degradation of SA during the experiments. The rate of SA production was calculated in these experiments by fitting the SA concentration to a zero-order production rate followed by a first-order degradation rate for SA.

The corresponding equation is derived in Text S3 (ESI) and an example of fitting is provided in Figure S8 (ESI).

Concomitantly to the FFA or BA irradiation experiments, we ran chemical actinometry daily to determine the irradiance of the lamps in the reactor. We used the PNA + pyridine actinometer at a concentration of 10 μM of PNA and of 5 mM of pyridine.(33) At this pyridine concentration, the quantum yield for the phototransformation of PNA (which depends on the pyridine concentration) is 1.74×10^{-3}.(34) All results were normalized by using the daily measured PNA phototransformation rate to the average PNA phototransformation value of 8.68×10^{-4} s^{-1}. The photon fluence rate in the interval λ= 340-410nm was calculated to be of 1.40×10^{-3} einstein m^{-2} s^{-1}.

Calculation of optical parameters

Optical parameters calculated from the UV-Vis absorption spectra are often used because absorption spectra are easy to measure and the optical parameters correlate with DOM properties that are harder to measure such as Φ_{1O2} and $\Phi_{\bullet OH}$. Several optical parameters were calculated using the measured UV-Vis absorbance spectra of the solutions. The specific UV absorbance $SUVA_{254}$ (unit L mg_C^{-1} m^{-1}) was calculated by dividing the absorbance at the wavelength λ=254nm by the carbon concentration ($5mg_C$ L^{-1}). Fitting a single-parameter exponential regression to the absorbance spectra in the wavelength range 300-600nm, the spectral slope (S, unit nm^{-1}) was calculated as the coefficient of the exponential fit (according to equation 6) using $Abs_{\lambda=350nm}$ as a constant. The *E2/E3* ratio was calculated as the ratio of the absorbance values at the wavelengths λ=250 over λ=365nm. Both the spectral slope and the E2/E3 ratio inversely correlate with the molecular weight of the DOM and positively correlate with Φ_{1O2} and $\Phi_{\bullet OH}$.(35-37) The wavelength averaged specific absorption coefficient ($SUVA_{avg}$, unit L mg_C^{-1} m^{-1}), which

is a proxy for the amount of light absorbed by the solutions, was calculated in the wavelength interval 340-410 nm according to equation 7, where $SUVA_\lambda$ is the specific absorption coefficient at a wavelength λ (unit L mg_C^{-1} m^{-1}) and I_λ is the normalized photon irradiance of the Rayonet reactor.

$$Abs_\lambda = Abs_{\lambda = 350\text{nm}}\, e^{-S(\lambda - 350nm)} \quad (6)$$

$$SUVA_{\text{avg}} = \frac{\int_{340nm}^{410nm} SUVA_\lambda I_\lambda d\lambda}{\int_{340nm}^{410nm} I_\lambda d\lambda} \quad (7)$$

Standard deviation

The standard deviations were calculated for the first-order degradation curves of FFA and PNA and for the zero-order production lines for SA and propagated from there. The error on the rate constants from the literature used in the calculations were also incorporated in the error calculation. The standard errors calculated for FFA degradation and SA production were used in addition to the standard errors for $SUVA_{\text{avg}}$ in the calculation of Φ_{1O2} and $\Phi_{\bullet OH}$. The standard errors for $SUVA_{\text{avg}}$ were calculated as the standard deviation of triplicate UV-Vis absorbance measurements of the DOM solutions and propagated from there. Examples of calculations are shown in Text S4 (ESI).

Results and discussion

Effects of ozonation on the optical properties of DOM

Absorption properties

As shown previously, ozonation induces a large decrease in the UV-Vis absorption of the two DOM isolates tested in this study (Figure 1). The allochthonous SRFA absorbs more light because it has a higher content of aromatic moieties than PLFA. While the absolute difference ($A_{O3\ dose=0}$-$A_{O3,dose}$) of the absorbance is more important at shorter wavelengths (Figures 1C and D), the relative decrease ($A_{O3}/A_{O3=0}$) in absorbance is smaller at shorter wavelengths (Figures 1E and D). Upon ozonation, the relative decrease in absorbance ($A_{O3}/A_{O3=0}$) differs for the two DOM types (Figures 1E and D). For PLFA, the relative decrease is more significant at longer wavelengths, whereas for SRFA the wavelength dependence is relatively small (see Figure S2, ESI). Typically, small ozone doses induce a large decrease in absorbance (Figures 1 and S2). For SRFA at λ=254 nm, the absorbance decreases by 52% for a specific ozone dose of 0.2 $mmol_{O3}$ $mmol_C^{-1}$ while for PLFA the decrease is 63%.

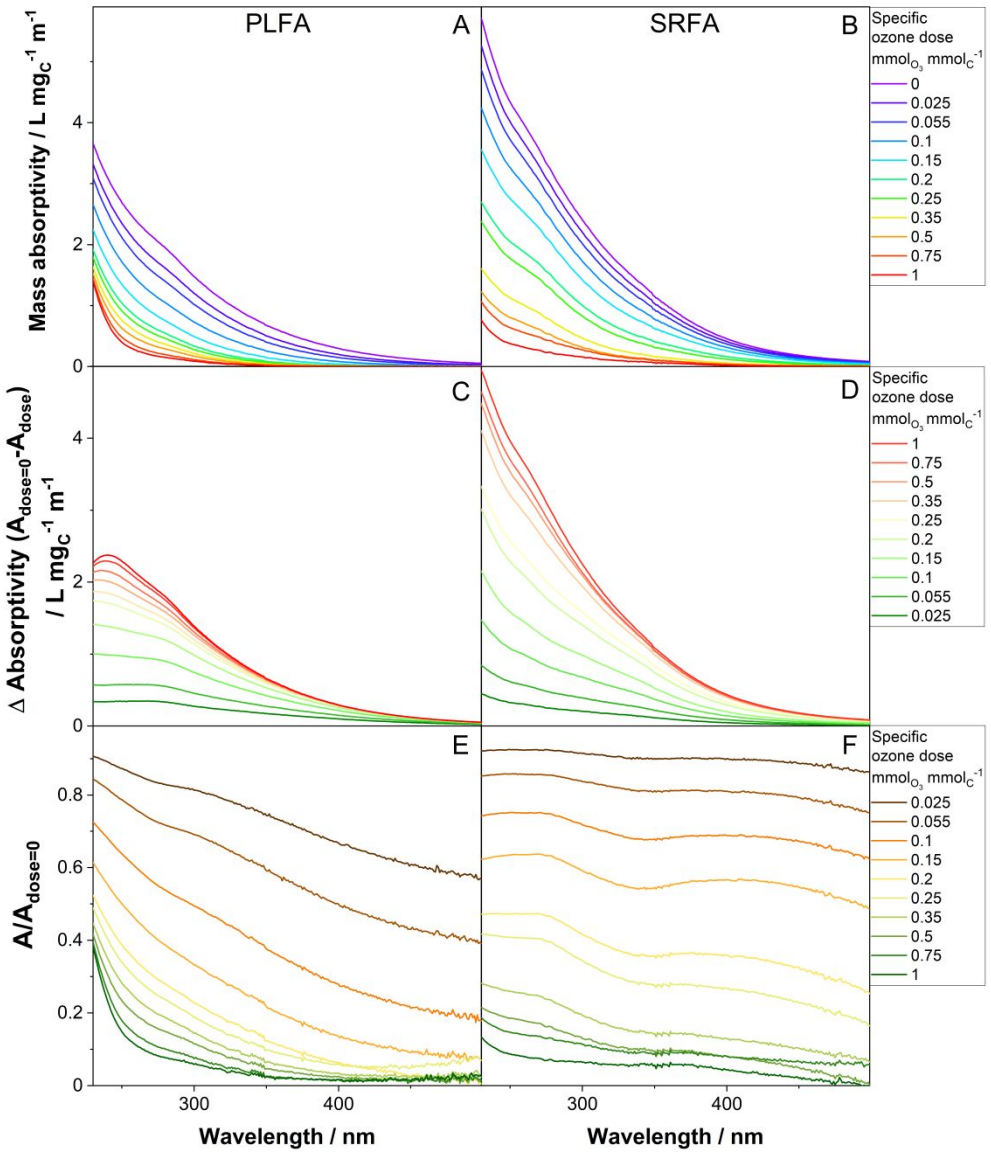

211

212 **Figure 1**. Effects of the specific ozone doses on the absorbance spectra of the two DOM samples
213 Pony Lake and Suwannee River fulvic acid (PLFA and SRFA respectively). (A) and (B): Mass
214 absorptivity as a function of the specific ozone dose for (A) PLFA, and (B) SRFA. (C) and (D):
215 variation of the mass absorptivity ($A_{O3,dose=0}$-$A_{O3,dose}$) as a function of the specific ozone dose for
216 (C) PLFA and (D) SRFA. (E) and (F): Ratio of the absorptivity ($A_{O3,dose}/A_{O3,dose=0}$) as a function
217 of the specific ozone dose for (E) PLFA and (F) SRFA. The samples were buffered at pH 7 using
218 10 mM phosphate buffer, with a DOM concentration of 5mg_C L^{-1}.

219

220 The observed effects of ozone on the absorption properties of DOM for specific ozone

221 doses of up to 0.2 $mmol_{O3}$ $mmol_C^{-1}$ are similar to a previous study conducted with the same

DOM types in presence of a •OH scavenger (as seen by similar reduction in $SUVA_{254}$, $SUVA_{280}$ and $SUVA_{350}$ values, see Figure S3, ESI)(3) and are similar to what was observed for three specific ozone doses for the same DOM types in the absence and presence of a •OH scavenger.(5) These observations can be mainly rationalized by the reaction of ozone with highly reactive activated aromatic compounds such as phenols. For specific ozone doses > 0.2 $mmol_{O3}$ $mmol_C^{-1}$, the extent of $SUVA_{254}$ decrease was higher in the current study compared to our previous investigation.(3) This can be attributed to a depletion of the pool of highly ozone-reactive chromophores for specific ozone doses > 0.2 $mmol_{O3}$ $mmol_C^{-1}$ and the reactions of •OH with these chromophores, which is possible due to the absence of a •OH scavenger. Such chromophores can be non-activated aromatic moieties such as benzene or methylated benzenes, which have low second order rate constants for the reactions with ozone but are highly reactive towards •OH ($k_{•OH,benzene}$ = 3.3×10^9 M^{-1} s^{-1}).(38) The reaction of benzene with •OH produces phenol, which then reacts quickly with ozone.

Optical parameters

Optical parameters such as $SUVA_{254}$, the ratio *E2*/*E3*, and the spectral slope are often calculated from the UV-Vis absorbance spectra for the characterization of waters.(35) In turn, these parameters are used to develop correlations with other reactivity measures of DOM, including the photochemical formation of $^1O_2$ or •OH as well as other properties such as aromaticity and molecular weight. (37, 39-41) Changes in these parameters are presented in Figure S4 (ESI) as a function of the specific ozone dose. A marked decrease in $SUVA_{254}$ with increasing specific ozone dose can be observed for both SRFA and PLFA (Figure S4A, ESI). In contrast, an increase in both the ratio *E2*/*E3* and the spectral slope can be observed for increasing

specific ozone doses (Figures S4B and C, ESI), respectively), being more pronounced for PLFA than for SRFA.

The results for ozonation in the presence and absence of an •OH scavenger (*t*-butanol) also show that the decrease in $SUVA_{254}$ and the increases in *E2*/*E3* and the spectral slope are more important for PLFA in absence of an •OH scavenger (Figure S4, ESI). For SRFA, $SUVA_{254}$ behaves similarly, however, for *E2*/*E3* and the spectral slope the observed increases are more pronounced in presence of the •OH scavenger. The spectral slope PLFA results are in contradiction with the results presented in ref. (5) where the absence of the •OH scavenger produced the opposite effect. The observed difference could be attributed to differences in the experimental conditions, with different DOM concentrations (10 $mg_C\ L^{-1}$ in ref. (5) vs 5 $mg_C\ L^{-1}$ in the current study) and a difference in the way the ozonation experiments was conducted (in ref. (5) the residual ozone was quenched after 2 hours vs 2 days in the present experiments).

As aforementioned, the $SUVA_{254}$, the ratio *E2*/*E3*, and the spectral slope correlate with $\Phi_{\bullet OH}$ and $\Phi_{^1O_2}$. These correlations are presented in Figure S5 and Table S2 (ESI). The slopes of the $\Phi_{^1O_2}$ regressions (Figures S5A-C) are comparable (factor 2) to our previous study with the same isolates in the presence of a •OH scavenger and to Everglades DOM (Table S2, ESI).(3, 37) The slopes of the $\Phi_{\bullet OH}$ regressions in this study are significantly larger (by a factor of 2-6) than that of the Everglades DOM.(37) This observed difference in slope for the $\Phi_{\bullet OH}$ regressions makes the direct use of any of the parameters ($SUVA_{254}$, the ratio *E2*/*E3*, and the spectral slope) as predictors of $\Phi_{\bullet OH}$ questionable. The difference in slope may reflect a change in DOM chemical composition due to ozonation, as opposed to DOM composition of the Everglades DOM.

Effects of ozonation on the photochemical generation of $^1O_2$ from DOM

The extent of light absorbed in the wavelength interval 340-410 nm by the two DOM isolates can be characterized by $SUVA_{avg}$ as a proxy, which decreases in an exponential-like fashion upon ozonation (Figure 2A). The steady-state concentration of $^1O_2$ produced upon UV irradiation (centered at λ=366 nm, see Figure S1, ESI) increases slightly for low specific ozone doses (0 to 0.1 $mmol_{O3}$ $mmol_C^{-1}$) and then decreases sharply (by a factor of 3) for PLFA and moderately for SRFA (Figure 2B). Because $[^1O_2]_{ss}$ is decreasing relatively less compared to $SUVA_{avg}$ (Figure 2A) it can be concluded that Φ_{1O2} (i.e., the ratio of the production of $^1O_2$ over the extent of light absorption) should increase with increasing specific ozone doses. This is illustrated in Figure 2C, where Φ_{1O2} increases close to linearly with increasing specific ozone doses. The increase in Φ_{1O2} is more significant for PLFA, with an increase from 1.9% (non-ozonated) to 13.1% (0.5 $mmol_{O3}$ $mmol_C^{-1}$), than for SRFA for which an increase from 1.0 to 8.5% for the same specific ozone doses was observed.

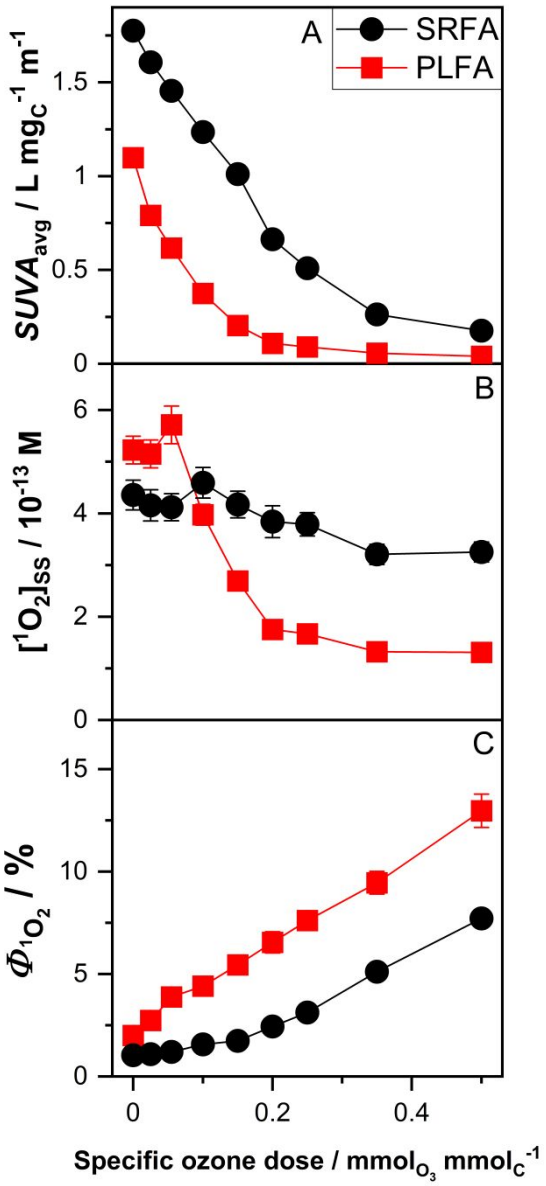

279

280 **Figure 2**. Effects of specific ozone doses on (A) the light absorption, (B) the generation of
281 singlet oxygen ($^1O_2$) and (C) the $^1O_2$ quantum yields (Φ_{1O2}) for Pony Lake and Suwannee River
282 fulvic acids (PLFA and SRFA, respectively). (A) Specific UV-Vis absorption ($SUVA_{avg}$) in the
283 wavelengths range 340-410 nm. (B) Measured steady-state $^1O_2$ concentration ($[^1O_2]_{ss}$) as a
284 function of the specific ozone doses. (C) $^1O_2$ quantum yield (Φ_{1O2}) as a function of the specific
285 ozone dose. Red squares/lines: PLFA; black circles/lines: SRFA, at a concentration of $5mg_C$ L^{-1}.
286 Solutions were buffered with 10 mM phosphate at pH 7, without hydroxyl radical scavenger.
287 Error bars represents standard errors in (B) and (C) were obtained from pseudo-first order fittings
288 (FFA experiments in duplicate). Lines are shown to guide the eye.
289

290 Increases in Φ_{1O2} were similar in a previous study on wastewater ozonation (13) and in a
291 study with the same DOM isolates but in the presence of a •OH scavenger (3) (see Figure S7,
292 ESI) for a comparison with the data from ref. (3)). The Φ_{1O2} values were 3.2 ± 0.4 % for the non-
293 ozonated wastewater and increased to 9.3 ±1.8 % for a specific ozone dose of 0.25 $mmol_{O3}$
294 $mmol_C^{-1}$,(13) which is similar to the observations for PLFA. For ozonation of the same DOM
295 isolates in presence of an •OH scavenger, Φ_{1O2} also increased close to linearly for low specific
296 ozone doses (< 0.35 $mmol_{O3}$ $mmol_C^{-1}$) but leveled off for higher specific ozone doses.(3) This
297 increase in Φ_{1O2} was attributed to the formation of quinones from the reaction of ozone with
298 phenolic DOM moieties and the observed increase of Φ_{1O2} in Figure 2 can most likely also be
299 attributed to a formation of quinones.

300 The normalized (to the non-ozonated experiment) Φ_{1O2} in this study was compared to the
301 data from ref. (3), where the ozonation was carried out in the presence of an •OH scavenger (see
302 Figure S7, ESI). The ratio of Φ_{1O2} from this study and the data from ref. (3) for PLFA is close to
303 1 for specific ozone doses up to 0.35 $mmol_{O3}$ $mmol_C^{-1}$ and increases to 1.5 for a specific ozone
304 dose of 0.5 $mmol_{O3}$ $mmol_C^{-1}$ (see Figure S7, ESI). To determine if this specific ozone dose was
305 anomalous, Φ_{1O2} was examined in detail by compiling the corresponding extent of $^1O_2$
306 production and extent of light absorption as a function of the ozone dose (see Table S3, ESI).
307 The increase to a value of 1.5 for a specific ozone dose of 0.5 $mmol_{O3}$ $mmol_C^{-1}$ can be attributed
308 to a decrease in the extent of $^1O_2$ production.(3) Ref. (3) presents additional specific ozone doses,
309 which confirm that this observation is reproducible. Therefore, the observed value of a ratio of
310 1.5 observed in Figure S7 (ESI) is not an outlier. For SRFA, the ratio decreases to a value of 0.7
311 for specific ozone doses up to 0.15 $mmol_{O3}$ $mmol_C^{-1}$ and then increases to 1.5 for specific ozone
312 doses between 0.15 and to 0.5 $mmol_{O3}$ $mmol_C^{-1}$.

313 The increase in the normalized quantum yield ratio to 1.5 for higher specific ozone doses
314 can likely be attributed to the reaction of •OH with non-activated aromatics, which are less
315 reactive to ozone. For the experiments in presence of a •OH scavenger, the pool of chromophores
316 that are non-reactive towards ozone are maintained and should overall have a lower Φ_{1O2} than
317 the pool of ozonated chromophores. Alternatively, in the present study in absence of a •OH
318 scavenger, the pool of ozone-resistant chromophores should react with •OH to produce phenols
319 and then quinones upon reaction with ozone,(15) which have a higher Φ_{1O2}.

Effects of ozonation on the •OH generation potential of DOM during UV irradiation

An approach similar to the Φ_{1O2} experiments was chosen to elucidate the factors influencing $\Phi_{\bullet OH}$ upon ozonation. The light absorbed by the two DOM types (quantified by $SUVA_{avg}$) decreases dramatically as a function of the specific ozone dose (Figure 2A). Figure 3A shows that the rate of •OH production upon irradiation, $r_{\bullet OH}$, is fairly constant with increasing specific ozone doses for PLFA, while for SRFA it first increases for specific ozone doses $\leq$ 0.2mmol$_{O3}$ mmol$_C^{-1}$ and then decreases for higher specific ozone doses. Because $SUVA_{avg}$ is decreasing while $r_{\bullet OH}$ remains fairly constant with increasing specific ozone doses, it can be concluded that $\Phi_{\bullet OH}$ is increasing, similarly to Φ_{1O2}. This is confirmed in Figure 3B, with a significant increase in $\Phi_{\bullet OH}$ for PLFA (by a factor of 28) and for SRFA (by a factor of 8.6) when the specific ozone dose increases from 0-0.5 mmol$_{O3}$ mmol$_C^{-1}$.

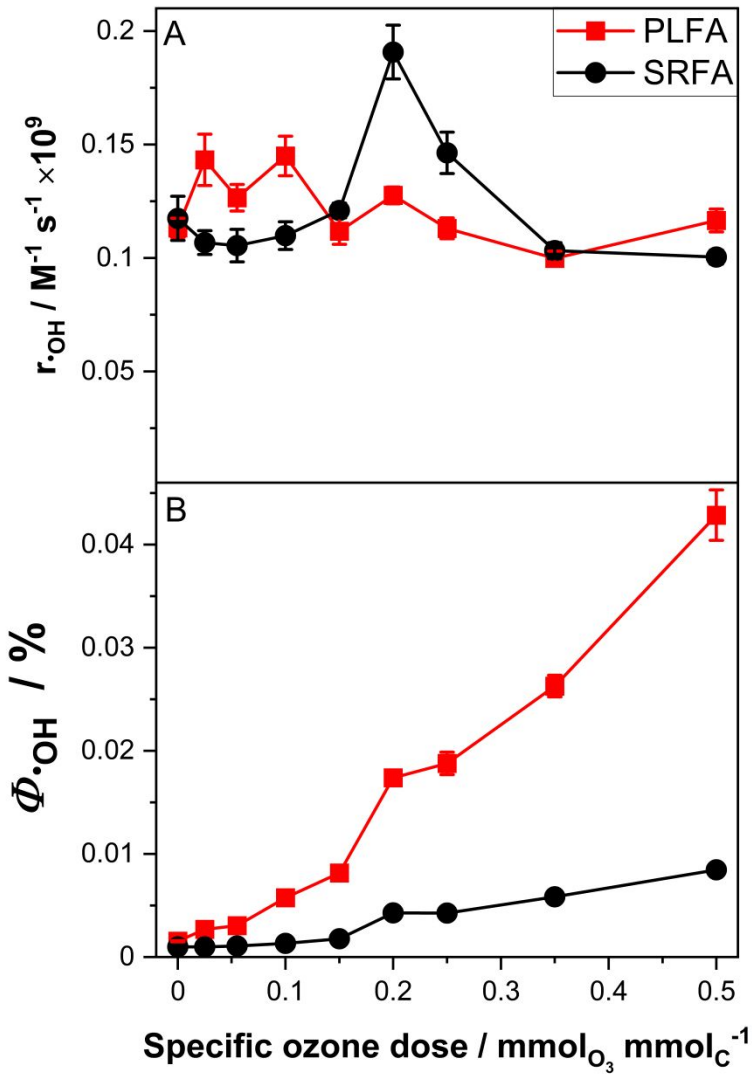

Figure 3. UV irradiation of DOM: Effects of the specific ozone dose on (A) the hydroxyl radical (•OH) production rate ($r_{\bullet OH}$) and (B) the •OH quantum yield ($\Phi_{\bullet OH}$) for Pony Lake and Suwannee River fulvic acid (PLFA and SRFA, respectively). Red squares/lines: PLFA; black circles/lines: SRFA at a concentration of $5 mg_C\ L^{-1}$. Solutions were buffered with 10 mM phosphate at pH 7, without hydroxyl radical scavenger. Error bars represent standard errors obtained from pseudo-first order fittings (BA experiments in duplicate). Lines are shown to guide the eye.

The formation pathway of •OH upon DOM irradiation is not entirely elucidated and many pathways have been proposed, which are summarized in a recent review.(11) Two main mechanisms are usually considered, H_2O_2-dependent and H_2O_2-independent pathways. The H_2O_2-dependent pathways involve Fenton and photo-Fenton chemistry and account for up to

50% of the •OH production in some samples.(42, 43) A variety of possibilities have been proposed for the H_2O_2-independent pathways. They include the photolysis of hydroxy substituted benzoic acids and phenols(44) and the oxidation of water or hydroxide ions by ^{3}DOM*, a mechanism that was seen to take place for a few photosensitizers such as 1-nitronaphthalene or anthraquinone-2,6-disulfonate.(45-47) If the production of •OH was due only to the photolysis of hydroxy substituted benzoic acids and phenols, one would expect $\Phi_{\bullet OH}$ to decrease upon ozonation due to the reaction and decomposition of the phenolic DOM moieties with ozone.(4, 15, 16, 48) The observed increase in $\Phi_{\bullet OH}$ indicates that the source of •OH is probably the oxidation of water or hydroxide ions by ^{3}DOM*, or the formation of H_2O_2 during ozonation, which could induce the H_2O_2-dependent pathway.

The one-electron oxidation potentials of water and hydroxide are -2.73 V and -1.90 V respectively.(49) Quinones are known to have a high intersystem crossing yield and under photoirradiation form triplets that have a one-electron reduction potential in the range of 2.2-2.4 V (9) which is high enough to react with hydroxide and potentially with water. Therefore, it is hypothesized that the observed increase in $\Phi_{\bullet OH}$ could be attributed to the formation of quinones, which are common products from the reactions of ozone with hydroxylated aromatic compounds (e.g., phenols). (4, 15, 16, 48) It should be noted that for non-ozonated DOM, the photolysis of hydroxy substituted benzoic acids and phenols should not be excluded as a •OH source. A scenario for which ozonation increases the •OH production from DOM quinone moieties and decreases the production of •OH from the photolysis of substituted benzoic acid and phenols is also possible.

In studies on the oxidation of water or hydroxide ions by ^{3}DOM*, it has been shown that some other hydroxylating species (•OH-like) are also generated, that have similar hydroxylating

366 properties as •OH but lower reactivity.(42) Experiments involving photosensitizers indicate that
367 some of them produce •OH(45, 50), but that for some photosensitizers, irradiation yielded
368 species that were assigned to sensitizer-water exciplexes that could potentially be •OH-like
369 species.(46, 51-53)
370 It should be noted that the probe used to quantify •OH in our experiments, BA, could potentially
371 also react with •OH-like species (42, 52) and that part of the •OH measured in the experiments
372 presented in Figure 3 could be caused by •OH-like species.
373
374 *Qualitative assessment of the production of •OH and of other hydroxylating species (•OH-like)*

375 To qualitatively assess the potential formation of •OH-like species upon DOM ozonation,
376 we designed the following competition kinetic experiment using BA as a probe and methanol as
377 an •OH scavenger (it should be noted that it is also possible to quantify the formation of •OH
378 using methanol but we only used it as a scavenger here). The assumption of these experiments is
379 that the ratio $\frac{k_{\mathrm{BA,\cdot OH}}}{k_{\mathrm{MeOH,\cdot OH}}}$ (where $k_{\mathrm{BA,\bullet OH}}$ =5.9×10^9 M^{-1} s^{-1} or $k_{\mathrm{MeOH,\bullet OH}}$ = 9.7×10^8 M^{-1} s^{-1} are the
380 second-order rate constants for the reactions between BA or methanol and •OH, respectively)(20)
381 will be different than the ratio $\frac{k_{\mathrm{BA,\bullet OH-like}}}{k_{\mathrm{MeOH,\bullet OH-like}}}$ (where $k_{\mathrm{BA,\bullet OH\text{-}like}}$ and $k_{\mathrm{MeOH,\bullet OH\text{-}like}}$ are the second-order
382 rate constants for the reactions between BA or methanol and •OH-like species, respectively). The
383 methanol quenching experiments were modeled using equation 8, where *f* is the fraction of •OH
384 reacting with BA, $k_{\mathrm{DOM,\bullet OH}}$ is the second-order constant between DOM and •OH (4.6×10^8 and
385 1.9×10^8 M$_C^{-1}$ s^{-1} for PLFA and SRFA respectively (54)) and $k_{\mathrm{NO2\text{-},\bullet OH}}$ is the second-order rate
386 constant for the reaction between nitrite and •OH (1×10^{10} M^{-1} s^{-1} (20)).

387 $$f = \frac{k_{\mathrm{BA,\bullet OH}}[\mathrm{BA}]}{k_{\mathrm{BA,\bullet OH}}[\mathrm{BA}] + k_{\mathrm{MeOH,\bullet OH}}[\mathrm{MeOH}] + k_{\mathrm{DOM,\bullet OH}}[\mathrm{DOM}] + k_{\mathrm{NO_2^-,\bullet OH}}[\mathrm{NO_2^-}]} \quad (8)$$

Note that the reactions of •OH with the phosphate buffer and carbonate/bicarbonate from atmospheric CO_2 were neglected, as the fractional consumption of •OH by these components was small (f value <0.0001 for the phosphate buffer and <0.01 for the carbonate/bicarbonate, considering saturation conditions at 20°C for the carbonate/bicarbonate concentration).

A control experiment was performed where nitrite was used as an alternative source of •OH to confirm the validity of equation 8 and to verify that methanol acts as an ideal quencher (a potential drawback of the use of methanol is that its reaction with •OH produces $O_2^{\bullet-}$ quantitatively,(1) and $O_2^{\bullet-}$ disproportionation forms H_2O_2 that is potentially an additional source of •OH in the system).

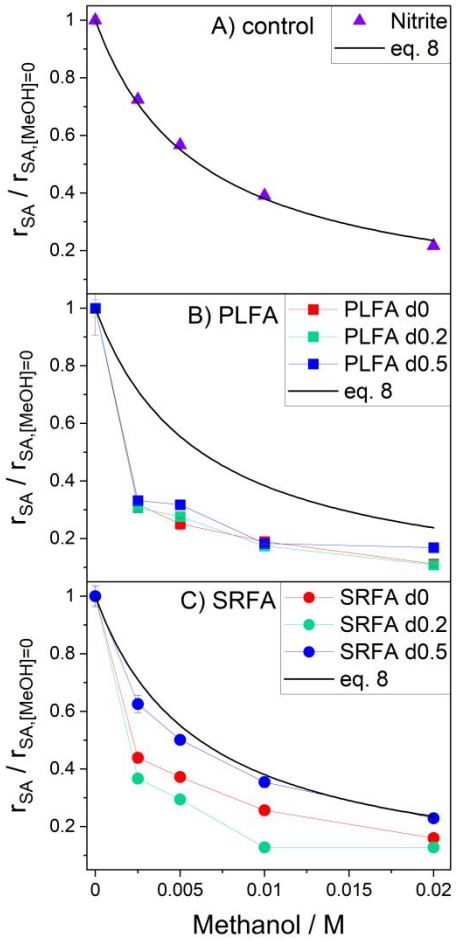

Figure 4. Normalized salicylic acid (SA) production rate as a function of the methanol concentration. (A) Control nitrite experiment (violet, 6µM $NaNO_2$). (B) Pony Lake Fulvic Acid

(PLFA) treated with specific ozone doses of 0, 0.2 and 0.5 $mmol_{O3}$ $mmol_{C}^{-1}$. (C) Suwannee River Fulvic Acid (SRFA) treated with specific ozone doses of 0, 0.2 and 0.5 $mmol_{O3}$ $mmol_{C}^{-1}$. The black lines represent the fraction of •OH reacting with BA according to Eq. 8. Benzoic acid concentration 1mM, carbon concentration $5mg_{C}$ L^{-1}. Solutions were buffered with 10 mM phosphate at pH 7. Lines are shown to guide the eye.

Figure 4 presents the normalized (to [methanol]=0) rate of SA production. Figure 4A shows that equation 8 accurately describes the experiments performed with the photolysis of nitrite as a source of •OH. In Figures 4B and 4C, a deviation from equation 8 is observed, indicating that BA is not only reacting with •OH in the system. In contrast, •OH-like species might also be produced and involved in BA abatement. The ratio of the calculated value from equation 8 over the experimental value is 1 for the nitrite control experiment. For PLFA the ratio is fairly constant for all specific ozone doses with a mean value of 0.47 for the non-ozonated samples and 0.46 and 0.55 for specific ozone doses of 0.2 and 0.5 $mmol_{O3}$ $mmol_{C}^{-1}$, respectively. For SRFA the ratio is 0.66 for the non-ozonated samples and 0.48 and 0.92 for specific ozone doses of 0.2 and 0.5 $mmol_{O3}$ $mmol_{C}^{-1}$, respectively.

The results for non-ozonated PLFA and SRFA can be compared to studies in which methane was used as a probe that is specific for •OH and non-reactive towards •OH-like species.(42) Methane quenching experiments indicate that for PLFA both •OH and •OH-like species are produced, while for SRFA •OH is produced.(42) One reason for this discrepancy might be the unknown sensitivity of terephthalic acid used in ref. (42) towards •OH-like species. This might not capture the full extent of •OH-like species produced in the SRFA experiments in ref. (42).

Comparison between the effects of ozonation on the generation potential of $^1O_2$ and $^{\bullet}OH$ during UV irradiation.

The measured Φ_{1O2} values were approximatively two orders of magnitude higher than $\Phi_{\bullet OH}$. This reflects the fact that $^1O_2$ is formed by oxygen reacting with ^{3}DOM* (eq. 3) with an efficiency that was evaluated to be approximately 30% (55), while $^{\bullet}$OH can be formed through several pathways that are relatively inefficient (vide supra).

A comparison of Φ_{1O2} and $\Phi_{\bullet OH}$ (Figure 5) shows that the two quantum yields increase significantly with increasing specific ozone doses. Figure 5A shows that $\Phi_{\bullet OH}$ and Φ_{1O2} increase more for PLFA than for SRFA. Plotting $\frac{\Phi_{\bullet OH,O_3}}{\Phi_{\bullet OH,O_3=0}} \Big/ \frac{\Phi^1{O_2,O_3}}{\Phi^1{O_2,O_3=0}}$ (i.e., the relative ratio of increases of the two quantum yields; Figure 5B) indicates that for PLFA, the increase in $\Phi_{\bullet OH}$ is more important than for Φ_{1O2}, while for SRFA the ratio of increase of the two quantum yields is near unity for most specific ozone doses except for 0.2 and 0.25 $mmol_{O3}$ $mmol_C^{-1}$, where higher ratios were observed.

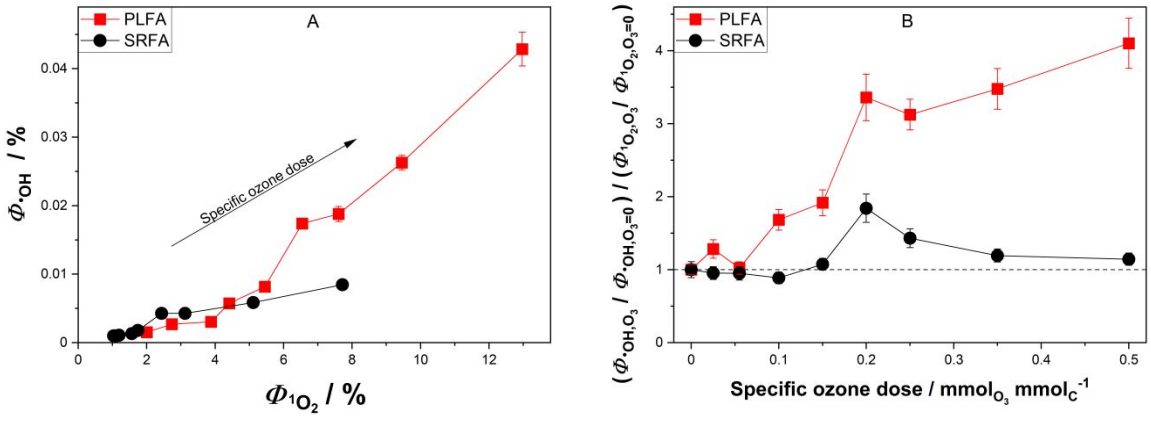

Figure 5. Comparison between the effects of ozonation on the hydroxyl radical quantum yield ($\Phi\bullet_{OH}$) and the singlet oxygen quantum yield (Φ_{1O2}) for Pony Lake and Suwannee River fulvic acids (PLFA and SRFA, respectively). (A) $\%\Phi\bullet_{OH}$ vs $\%\Phi_{1O2}$. (B) Ratio of the normalized (to a

specific ozone dose of 0 $mmol_{O3}$ $mmol_{C}^{-1}$) $\Phi\bullet_{OH}$ over the normalized (to a specific ozone dose of 0 $mmol_{O3}$ $mmol_{C}^{-1}$) Φ_{1O2} as a function of the specific ozone dose. Red squares/lines: PLFA; black circles/lines: SRFA. DOM at concentrations of $5mg_{C}$ L^{-1}. Solutions were buffered with 10 mM phosphate at pH 7, without hydroxyl radical scavenger. Error bars represent standards errors obtained from the pseudo-first order fittings (FFA or BA experiments in duplicate). Lines are shown to guide the eye.

The observed increase in Φ_{1O2} was attributed to the formation of quinones from the ozonation of phenolic DOM moieties. Only a relatively small subset of DOM chromophores produces •OH. The relative increase in $\Phi_{\bullet OH}$ is related to either a selective destruction of DOM chromophores that do not produce •OH or the formation of new DOM moieties that can produce •OH. An example of such new DOM moieties is quinones that are formed during ozonation and that under photoirradiation form triplets that have potentially high enough triplet one-electron oxidation potential to form •OH from water or hydroxide ions (see above).

Based on the current understanding of DOM photochemistry, it is difficult to develop an overarching model that explains the results observed in this study, as well as in other investigations by the authors. It is possible that the results observed in this study are explained by the recalcitrance of quinone-derivatives to transformation by ozone and •OH. However, it is not clear if the photochemistry of quinones results in direct •OH formation or the formation of •OH-like species and the relative efficiency of these two processes. It is also not clear how hydroxylation of quinones would affect $^1O_2$ formation.

In a previous study, we had also observed a positive correlation between the fluorescence quantum yield and the yield for the formation of $^1O_2$ during pre-ozonation in the presence of an •OH scavenger.(3) Although we did not measure the fluorescence quantum yield in the current study, we expect that the same positive relationship would apply. Given that quinones are not

fluorescent, it is unclear whether these observed correlations have any causational basis. More work is needed to ascertain these intercorrelations.

Conclusion

This study focused on the effects of ozonation on the optical and photochemical properties of two DOM types. Ozonation induced a significant decrease in DOM light absorbance properties and significant increases in the quantum yields of singlet oxygen ($\Phi_{^1O_2}$) and hydroxyl radical ($\Phi_{^\bullet OH}$). For SRFA, the $\Phi_{^\bullet OH}$ was observed to increase similarly to $\Phi_{^1O_2}$, while for PLFA the increase in $\Phi_{^\bullet OH}$ was approximately a factor four larger than the observed increase in $\Phi_{^1O_2}$. The increases in $\Phi_{^1O_2}$ and $\Phi_{^\bullet OH}$ were linked to the reactions of phenolic DOM moieties with ozone, which lead to the formation of quinones. The simultaneous use of a $^\bullet$OH probe and a $^\bullet$OH scavenger allowed for the distinction between the formation of $^\bullet$OH and of other hydroxylating species ($^\bullet$OH-like species).

Overall, ozonation leads to an important decrease in the light absorption properties of DOM, which makes it a useful pre-treatment for UV-based treatment since the transparency of the water increases. For municipal wastewaters, where ozonation is used as a polishing step before discharge, the results of this study indicate that ozonation improves the visual aesthetics of the treated wastewater and also increases the potential for $^1O_2$- and $^\bullet$OH-induced reactions.

Acknowledgements

Funding for this study came from the US National Science Foundation (1808126, 1833421, and 1549387). Funding from the University of Colorado SMART and Discovery Learning Assistantships programs is also acknowledged.

Associated Content

Electronic supplementary information

Electronic supplementary information (ESI) available. See DOI:

Author information

Corresponding author

*E-mail: Fernando.rosario@colorado.edu

ORCID

Frank Leresche: 0000-0001-8400-3142

Jeremy Torres-Ruiz: 0000-0003-4331-7991

Tyler Kurtz: 0000-0001-6310-3240

Urs von Gunten: 0000-0001-6852-8977

Fernando Rosario-Ortiz: 0000-0002-3311-9089

Note

The authors declare no competing financial interest.

References

1. von Sonntag, C.; von Gunten, U.; C*hemistry of Ozone in Water and Wastewater Treatment: From Basic Principles to Applications*; IWA Publishing: London, UK, **2012**.
2. Eggen, R. I.; Hollender, J.; Joss, A.; Scharer, M.; Stamm, C., Reducing the Discharge of Micropollutants in the Aquatic Environment: the Benefits of Upgrading Wastewater Treatment Plants. *Environ. Sci. Technol.* **2014,** *48* (14), 7683-9.
3. Leresche, F.; McKay, G.; Kurtz, T.; von Gunten, U.; Canonica, S.; Rosario-Ortiz, F. L., Effects of Ozone on the Photochemical and Photophysical Properties of Dissolved Organic Matter. *Environ. Sci. Technol.* **2019,** *53* (10), 5622-5632.
4. Önnby, L.; Salhi, E.; McKay, G.; Rosario-Ortiz, F. L.; von Gunten, U., Ozone and Chlorine Reactions with Dissolved Organic Matter - Assessment of Oxidant-Reactive Moieties by Optical Measurements and the Electron Donating Capacities. *Water Res.* **2018,** (144), 64-75.
5. Wenk, J.; Aeschbacher, M.; Salhi, E.; Canonica, S.; von Gunten, U.; Sander, M., Chemical Oxidation of Dissolved Organic Matter by Chlorine Dioxide, Chlorine, and Ozone: Effects on its Optical and Antioxidant Properties. *Environ. Sci. Technol.* **2013,** *47* (19), 11147-56.
6. Fono, L. J.; Kolodziej, E. P.; Sedlak, D. L., Attenuation of Wastewater-Derived Contaminants in an Effluent-Dominated River. *Environ. Sci. Technol.* **2006,** *40* (23), 7257-7262.
7. Link, M.; von der Ohe, P. C.; Voss, K.; Schafer, R. B., Comparison of Dilution Factors for German Wastewater Treatment Plant Effluents in Receiving Streams to the Fixed Dilution Factor from Chemical Risk Assessment. *Sci. Total Environ.* **2017,** *598*, 805-813.
8. Fenner, K.; Canonica, S.; Wackett, L. P.; Elsner, M., Evaluating Pesticide Degradation in the Environment: Blind Spots and Emerging Opportunities. *Science* **2013,** *341* (6147), 752-8.
9. McNeill, K.; Canonica, S., Triplet State Dissolved Organic Matter in Aquatic Photochemistry: Reaction Mechanisms, Substrate Scope, and Photophysical Properties. *Environ. Sci.-Process Impacts* **2016,** *18* (11), 1381-1399.
10. Richard, C.; Canonica, S., Aquatic Phototransformation of Organic Contaminants Induced by Coloured Dissolved Natural Organic Matter. In *Handbook of Environmental Chemistry*, Springer-Verlag, Berlin, Germany, **2005**; Vol. 2, pp 299-323.
11. Vione, D.; Minella, M.; Maurino, V.; Minero, C., Indirect Photochemistry in Sunlit Surface Waters: Photoinduced Production of Reactive Transient Species. *Chemistry* **2014,** *20* (34), 10590-606.
12. Hoigné, J.; Faust, B. C.; Haag, W. R.; Scully, F. E.; Zepp, R. G., Aquatic Humic Substances as Sources and Sinks of Photochemically Produced Transient Reactants. *Acs Adv. Chem. Ser.* **1989,** *219*, 363-381.
13. Mostafa, S.; Rosario-Ortiz, F. L., Singlet Oxygen Formation from Wastewater Organic Matter. *Environ. Sci. Technol.* **2013,** *47* (15), 8179-86.
14. Wert, E. C.; Rosario-Ortiz, F. L.; Drury, D. D.; Snyder, S. A., Formation of Oxidation Byproducts from Ozonation of Wastewater. *Water Res.* **2007,** *41* (7), 1481-1490.

15. Tentscher, P. R.; Bourgin, M.; von Gunten, U., Ozonation of *Para*-Substituted Phenolic Compounds Yields *p*-Benzoquinones, Other Cyclic *α,β*-Unsaturated Ketones, and Substituted Catechols. *Environ. Sci. Technol.* **2018,** *52* (8), 4763-4773.
16. Mvula E, von Sonntag C. Ozonolysis of phenols in aqueous solution. *Org. Biomol. Chem.* **2003**, 1(10), 1749-56.
17. Flyunt, R.; Leitzke, A.; Mark, G.; Mvula, E.; Reisz, E.; Schick, R.; von Sonntag, C., Determination of $^{\bullet}OH$, $O_2^{\bullet-}$, and Hydroperoxyde Yield in Ozone Reaction in Aqueous Solution. *J. Phys. Chem. B* **2003,** *107* (30), 7242-53.
18. Buffle, M. O.; von Gunten, U., Phenols and Amine Induced $HO^{\bullet}$ Generation During the Initial Phase of Natural Water Ozonation. *Environ. Sci. Technol.* **2006,** *40* (9), 3057-3063.
19. Nöthe, T.; Fahlenkamp, H.; von Sonntag, C., Ozonation of Wastewater: Rate of Ozone Consumption and Hydroxyl Radical Yield. *Environ. Sci. Technol.* **2009,** *43* (15), 5990-5.
20. Buxton, G. V.; Greenstock, C. L.; Helman, W. P.; Ross, A. B., Critical-Review of Rate Constants for Reactions of Hydrated Electrons, Hydrogen-Atoms and Hydroxyl Radicals ($^{\bullet}OH/^{\bullet}O^-$) in Aqueous-Solution. *J. Phys. Chem. Ref. Data* **1988,** *17* (2), 513-886.
21. Mártire D.O., Evans C, Bertolotti S.G., Braslavsky S.E., Garcia N.A. Singlet Molecular-Oxygen Production and Quenching by Hydroxybiphenyls. *Chemosphere.* **1993**, 26(9), 1691-701.
22. Wilkinson F, Helman W.P, Ross A.B. Quantum Yields for the Photosensitized Formation of the Lowest Electronically Excited Singlet-State of Molecular-Oxygen in Solution. *J. Phys. Chem. Ref. Data.* **1993**, 22(1), 113-262.
23. Schmidt R, Tanielian C, Dunsbach R, Wolff C. Phenalenone, a Universal Reference Compound for the Determination of Quantum Yield of Singlet Oxygen Sensitization *J. Photochem. and Photobiol. A-Chemistry*. **1994**, 79(1-2), 11-7.
24. Marti C, Jurgens O, Cuenca O, Casals M, Nonell S. Aromatic ketones as standards for singlet molecular oxygen photosensitization. Time-resolved photoacoustic and near-IR emission studies. J. Photochem. and Photobiol. A-Chemistry. **1996**, 97(1-2), 11-8.
25. Gutiérrez I, Bertolotti SG, Biasutti MA, Soltermann AT, Garcia NA. Quinones and hydroxyquinones as generators and quenchers of singlet molecular oxygen. *Canadian J. of Chem.-Revue Canadienne de Chimie*. **1997**,75(4),423-8.
26. Bourgin, M.; Beck, B.; Boehler, M.; Borowska, E.; Fleiner, J.; Salhi, E.; Teichler, R.; von Gunten, U.; Siegrist, H.; McArdell, C. S., Evaluation of a Full-Scale Wastewater, Treatment Plant Upgraded with Ozonation and Biological Post-Treatments: Abatement of Micropollutants, Formation of Transformation Products and Oxidation By-Products. *Water Res.* **2018,** *129*, 486-498.
27. Hollender, J.; Zimmermann, S. G.; Koepke, S.; Krauss, M.; McArdell, C. S.; Ort, C.; Singer, H.; von Gunten, U.; Siegrist, H., Elimination of Organic Micropollutants in a Municipal Wastewater Treatment Plant Upgraded with a Full-Scale Post-Ozonation Followed by Sand Filtration. *Environ. Sci. Technol.* **2009,** *43* (20), 7862-7869.
28. Zimmermann, S. G.; Wittenwiler, M.; Hollender, J.; Krauss, M.; Ort, C.; Siegrist, H.; von Gunten, U., Kinetic Assessment and Modeling of an Ozonation Step for Full-Scale Municipal Wastewater Treatment: Micropollutant Oxidation, By-Product Formation and Disinfection. *Water Res.* **2011,** *45* (2), 605-617.
29. Hammes, F.; Salhi, E.; Koster, O.; Kaiser, H. P.; Egli, T.; von Gunten, U., Mechanistic and Kinetic Evaluation of Organic Disinfection By-Product and Assimilable Organic

Carbon (AOC) Formation During the Ozonation of Drinking Water. *Water Res.* **2006,** *40* (12), 2275-2286.
30. Rosario-Ortiz, F. L., Canonica S., Probe Compounds to Assess the Photochemical Activity of Dissolved Organic Matter. *Environ. Sci. Technol.* **2016,** *50* (23), 12532-47.
31. Appiani, E.; Ossola, R.; Latch, D. E.; Erickson, P. R.; McNeill, K., Aqueous Singlet Oxygen Reaction Kinetics of Furfuryl Alcohol: Effect of Temperature, pH, and Salt Content. *Environ. Sci.-Process Impacts* **2017,** *19* (4), 507-516.
32. Qian, J. G.; Mopper, K.; Kieber, D. J., Photochemical Production of the Hydroxyl Radical in Antarctic Waters. *Deep-Sea Res. 1.* **2001,** *48* (3), 741-759.
33. Dulin, D.; Mill, T., Development and Evaluation of Sunlight Actinometers. *Environ. Sci. Technol.* **1982,** *16* (11), 815-20.
34. Laszakovits, J. R.; Berg, S. M.; Anderson, B. G.; O'Brien, J. E.; Wammer, K. H.; Sharpless, C. M., *p*-Nitroanisole/Pyridine and *p*-Nitroacetophenone/Pyridine Actinometers Revisited: Quantum Yield in Comparison to Ferrioxalate. *Environ. Sci. Technol. Lett.* **2017,** *4* (1), 11-14.
35. Peuravuori, J.; Pihlaja, K., Molecular Size Distribution and Spectroscopic Properties of Aquatic Humic Substances. *Anal. Chim. Acta* **1997,** *337* (2), 133-149.
36. Boyle E.S., Guerriero N, Thiallet A, Del Vecchio R, Blough N.V. Optical properties of humic substances and CDOM: relation to structure. *Environ. Sci. Technol.* **2009**, 43(7), 2262-8.
37. McKay, G.; Huang, W. X.; Romera-Castillo, C.; Crouch, J. E.; Rosario-Ortiz, F. L.; Jaffe, R., Predicting Reactive Intermediate Quantum Yields from Dissolved Organic Matter Photolysis Using Optical Properties and Antioxidant Capacity. *Environ. Sci. Technol.* **2017,** *51* (10), 5404-5413.
38. Dorfman L.M, Harter D.A., Taub I.A. Rate Constants for the Reaction of the Hydroxyl Radical with Aromatic Molecules. *J. Chem. Phys*. **1964**, 41(9), 2954-2955.
39. Helms, J. R.; Stubbins, A.; Ritchie, J. D.; Minor, E. C.; Kieber, D. J.; Mopper, K., Absorption Spectral Slopes and Slope Ratios as Indicators of Molecular Weight, Source, and Photobleaching of Chromophoric Dissolved Organic Matter. *Limnol. Oceanogr.* **2008,** *53* (3), 955-969.
40. Dalrymple, R. M.; Carfagno, A. K.; Sharpless, C. M., Correlations Between Dissolved Organic Matter Optical Properties and Quantum Yield of Singlet Oxygen and Hydrogen Peroxide. *Environ. Sci. Technol.* **2010,** *44*, 5824-5829.
41. Peterson, B. M.; McNally, A. M.; Cory, R. M.; Thoemke, J. D.; Cotner, J. B.; McNeill, K., Spatial and Temporal Distribution of Singlet Oxygen in Lake Superior. *Environ. Sci. Technol.* **2012,** *46* (13), 7222-9.
42. Page, S. E.; Arnold, W. A.; McNeill, K., Assessing the Contribution of Free Hydroxyl Radical in Organic Matter-Sensitized Photohydroxylation Reactions. *Environ. Sci. Technol.* **2011,** *45* (7), 2818-2825.
43. Dong, M. M.; Rosario-Ortiz, F. L., Photochemical Formation of Hydroxyl Radical from Effluent Organic Matter. *Environ. Sci. Technol.* **2012,** *46* (7), 3788-3794.
44. Sun, L. N.; Qian, J. G.; Blough, N. V.; Mopper, K., Insights into the Photoproduction Sites of Hydroxyl Radicals by Dissolved Organic Matter in Natural Waters. *Environ. Sci. Technol. Lett.* **2015,** *2* (12), 352-356.
45. Sur, B.; Rolle, M.; Minero, C.; Maurino, V.; Vione, D.; Brigante, M.; Mailhot, G., Formation of Hydroxyl Radicals by Irradiated 1-Nitronaphthalene (1NN): Oxidation of

635 Hydroxyl Ions and Water by the 1NN Triplet State. *Photochem. & Photobiol. Sc.* **2011,** *10*
636 (11), 1817-1824.
637 46. Moore, J. N.; Phillips, D.; Nakashima, N.; Yoshihara, K., Photochemistry of 9,10-
638 Anthraquinone-2,6-disulphonate. *J. Chem. Soc. Faraday Trans.* **1986,** *82*, 745-761.
639 47. Garg, S.; Rose, A. L.; Waite, T. D., Production of Reactive Oxygen Species on Photolysis
640 of Dilute Aqueous Quinone Solutions. *Photochem. Photobiol.* **2007,** *83* (4), 904-913.
641 48. Ramseier, M. K.; von Gunten, U., Mechanisms of Phenol Ozonation-Kinetics of Formation
642 of Primary and Secondary Reaction Products. *Ozone Sc. & Eng.* **2009,** *31* (3), 201-215.
643 49. Armstrong, D. A.; Huie, R. E.; Koppenol, W. H.; Lymar, S. V.; Merenyi, G.; Neta, P.;
644 Ruscic, B.; Stanbury, D. M.; Steenken, S.; Wardman, P., Standard Electrode Potentials
645 Involving Radicals in Aqueous Solution: Inorganic Radicals (IUPAC Technical Report).
646 *Pure Appl. Chem.* **2015,** *87* (11-12), 1139-1150.
647 50. Kitamura, T.; Fudemoto, H.; Wada, Y.; Murakoshi, K.; Kusaba, M.; Nakashima, N.;
648 Majima, T.; Yanagida, S., Visible Light Induced Photo-Oxidation of Water. Formation of
649 Intermediary Hydroxyl Radicals through the Photoexcited Triplet State of
650 Perfluorophenazine. *J. Chem. Soc. Faraday Trans.* **1997,** *93* (2), 221-229.
651 51. Gan, D.; Jia, M.; Vaughan, P. P.; Falvey, D. E.; Blough, N. V., Aqueous Photochemistry
652 of Methyl-benzoquinone. *J. Physical Chemistry A* **2008,** *112* (13), 2803-2812.
653 52. Pochon, A.; Vaughan, P. P.; Gan, D. Q.; Vath, P.; Blough, N. V.; Falvey, D. E.,
654 Photochemical Oxidation of Water by 2-Methyl-1,4-benzoquinone: Evidence Against the
655 Formation of Free Hydroxyl Radical. *J. Physical Chemistry A* **2002,** *106* (12), 2889-2894.
656 53. Loeff, I.; Treinin, A.; Linschitz, H., Photochemistry of 9,10-Anthraquinone-2-Sulfonate in
657 Solution. 1. Intermediates and Mechanism. *J. Physical Chemistry* **1983,** *87* (14), 2536-
658 2544.
659 54. Appiani, E.; Page, S. E.; McNeill, K., On the Use of Hydroxyl Radical Kinetics to Assess
660 the Number-Average Molecular Weight of Dissolved Organic Matter. *Environ. Sci.*
661 *Technol.* **2014**.
662 55. Schmitt, M.; Erickson, P. R.; McNeill, K., Triplet-State Dissolved Organic Matter
663 Quantum Yields and Lifetimes from Direct Observation of Aromatic Amine
664 Oxidation. *Environ. Sci. Technol.* **2017,** *51* (22), 13151-13160.

665

666

667

668

669 **Graphical Abstract**

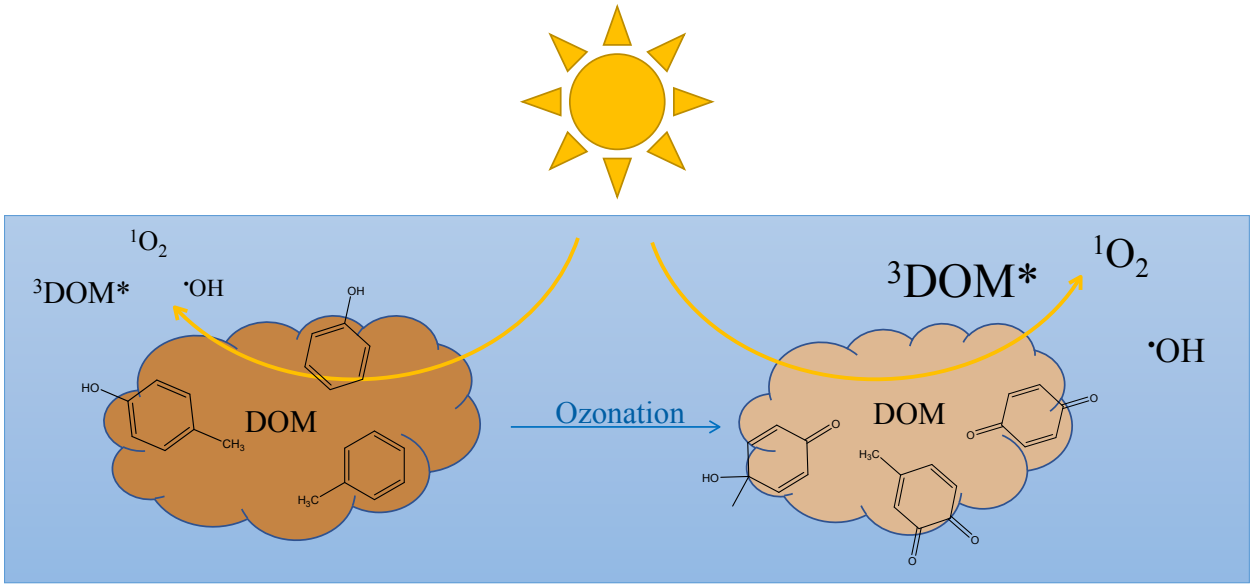

670
671

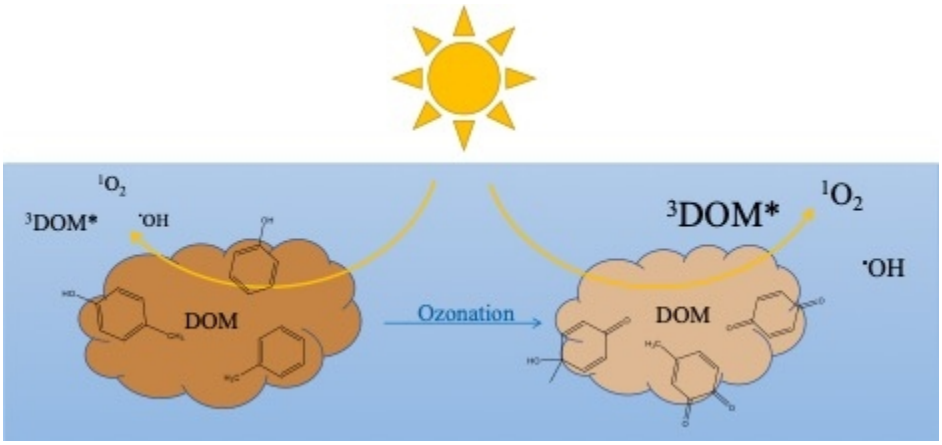

165x76mm (72 x 72 DPI)